Spintronics with NSN Junction of one-dimensional quantum wires: A study of Pure Spin Current and Magnetoresistance

Sourin Das[1], Sumathi Rao[2] and Arijit Saha[2]

[1] *Department of Condensed Matter Physics, Weizmann Institute of Science, Rehovot 76 100, Israel*
[2] *Harish−Chandra Research Institute, Chhatnag Road, Jhusi, Allahabad 211 019, India*

PACS 73.23.-b – Electronic transport in mesoscopic systems
PACS 74.45.+c – Proximity effects; Andreev effect; SN and SNS junctions
PACS 72.25.Ba – Spin polarized transport in metals

Abstract. - We demonstrate possible scenarios for production of pure spin current and large tunnelling magnetoresistance ratios from elastic co-tunnelling and crossed Andreev reflection across a superconducting junction comprising of normal metal-superconductor-normal metal, where, the normal metal is a one-dimensional interacting quantum wire. We show that there are fixed points in the theory which correspond to the case of pure spin current. We analyze the influence of electron-electron interaction and see how it stabilizes or de-stabilizes the production of pure spin current. These fixed points can be of direct experimental relevance for spintronics application of normal metal-superconductor-normal metal junctions of one-dimensional quantum wires. We also calculate the power law temperature dependence of the crossed Andreev reflection enhanced tunnelling magnetoresistance ratio for the normal metal-superconductor-normal metal junction.

Introduction. – Two fundamental degrees of freedom associated with an electron that are of direct interest to condensed matter physics are its charge and spin. Until very recently, all conventional electron-based devices have been solely based upon the utilization and manipulation of the charge degree of freedom of an electron. However, the realization of the fact that devices based on the spin degree of freedom can be almost dissipation-less and with very fast switching times, has led to an upsurge in research activity in this direction in recent years [1–3]. The first step towards realization of spin-based electronics (spintronics) would be to produce pure spin current (SC). From a purely theoretical point of view, it is straight forward to define a charge current as a product of local charge density with the charge velocity, but such a definition cannot be straight forwardly extended to the case of SC. This is because both spin $\vec{S}$ and velocity $\vec{v}$ are vector quantities and hence the product of two such vectors will be a tensor.

In this letter, we adopt the simple minded definition of SC, which is commonly used [4]. It is just the product of the local spin polarization density associated with the electron or hole, (a scalar s which is either positive for up-spin or negative for down-spin) and its velocity [4]. The most obvious scenario in which one can generate a pure SC in the sense defined above would be to have *(a)* an equal and opposite flow of identically spin-polarized electrons through a channel, such that the net charge current through the channel is nullified leaving behind a pure SC, or *(b)* alternatively, an equal flow of identically spin polarized electrons and holes in the same direction through a channel giving rise to pure SC with perfect cancellation of charge current. In this letter, we explore the second possibility for generating pure SC using a normal metal−superconductor−normal metal (NSN) junction.

Proposed device and its theoretical modelling. – The configuration we have in mind for the production of pure SC is shown in Fig. 1. The idea is to induce a pair potential in a small region of a quantum wire (QW) by depositing a superconducting strip on top of the wire (which may be, for instance, a carbon nanotube) due to proximity effects. If the strip width on the wire is of the order of the phase coherence length of the superconductor, then both direct electron to electron co-tunnelling as well as crossed Andreev electron to hole tunnelling can occur across the superconducting region [5]. It is worth pointing out that in the case of a singlet superconductor, which is the case we consider, both the tunnelling processes will conserve spin. In order to describe the mode of operation of the device (see Fig. 1), we first assume that the S-matrix rep-

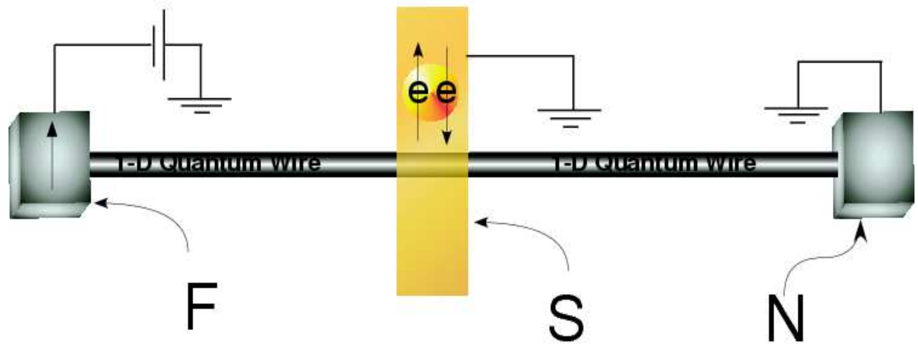

Fig. 1: A 1–D quantum wire (carbon nanotube) connected to a ferromagnetic (F) lead on the left and a normal (N) lead on the right. The thin strip in the middle of the wire depicts a 2–D layer of superconducting material deposited on top of the wire.

resenting the NSN junction described above respects parity symmetry about the junction, particle-hole symmetry and spin-rotation symmetry. Considering all the symmetries, we can describe the superconducting junction connecting the two half wires by an S-matrix with only four independent parameters namely, *(i)* the normal refection amplitude (r) for e (h), *(ii)* the transmission amplitude (t) for e (h), *(iii)* the Andreev reflection (AR) amplitude (r_A) for e (h), and *(iv)* the crossed Andreev reflection (CAR) amplitude (t_A) for e (h). If we inject spin polarized electron ($\uparrow$ e) from the left QW using a ferromagnetic contact and tune the junction parameters such that t and t_a are equal to each other, it will lead to a pure SC flowing in the right QW (see Fig. 1). This is so because, on an average, an equal number of electrons ($\uparrow$ e) (direct electron to electron tunnelling) and holes ($\uparrow$ h) (crossed Andreev electron to hole tunnelling) are injected from the left wire to the right wire resulting in production of pure SC in the right wire. Note that spin up holes ($\uparrow$ h) implies a Fermi sea with an absence of spin down electron (which is what is needed for the incident electron ($\uparrow$ e) to form a Cooper pair and enter the singlet superconductor).

Renormalisation Group study. – We now include the effects of inter-electron interactions on the S-matrix using the renormalisation group (RG) method introduced in Ref. [6]. This was furthur generalized to the case of multiple wires in Refs. [7,8] and to the case of 1–D NS junction [9–11]. The basic idea of the method is as follows. The presence of scattering (reflection) induces Friedel oscillations in the density of non-interacting electrons. Within a mean field picture for a weakly interacting electron gas, the electron not only scatters off the potential barrier but also scatters off these density oscillations with an amplitude proportional to the interaction strength. Hence by calculating the total reflection amplitude due to scattering from the scalar potential scatterer and from the Friedel oscillations created by the scatterer, we can include the effect of electron-electron interaction in calculating transport. This approach can be generalized to junctions of one-dimensional (1–D) QW with a single superconductor. In this case, there will be non-zero AR in the bulk of the wire due to proximity induced pair potential, besides the AR right at the NSN junction which turns an incoming electron into an outgoing hole.

The RG equations for a NS case have been obtained earlier using bosonization [12–14] and using WIRG [9,11]. In this letter we extend these WIRG results to the NSN case. To obtain the RG equations in the presence of AR and CAR for the NSN junction, we follow a procedure similar to that used in Ref. [7]. The fermion fields expanded around the left and right Fermi momenta on each wire can be written as, $\psi_{is}(x) = \Psi_{I\,is}(x)\, e^{i\,k_F\,x} + \Psi_{O\,is}(x)\, e^{-i\,k_F\,x}$; where i is the wire index, s is the spin index which can be $\uparrow,\downarrow$ and $I(O)$ stand for incoming (outgoing) fields. Note that $\Psi_{I(O)}(x)$ are slowly varying fields on the scale of k_F^{-1}. For a momentum in the vicinity of k_F, the incoming and outgoing fields can be Fourier expanded as:

$$\begin{aligned}\Psi_{ks}(x) \;=\; &\int dk\,\Big[b_{ks}\,e^{i\,(k+k_F)\,x} + d^{\dagger}_{ks}\,e^{i\,(-k+k_F)\,x} \\ &+ r\,b_{ks}\,e^{-i\,(k+k_F)\,x} + r^{\star}\,d^{\dagger}_{ks}\,e^{-i\,(-k+k_F)\,x} \\ &+ r_A\,d_{ks}\,e^{-i\,(-k+k_F)\,x} + r^{\star}_A\,b^{\dagger}_{ks}\,e^{-i\,(k+k_F)\,x}\Big]\end{aligned} \tag{1}$$

where b_{ks} is the electron destruction operator and d_{ks} is the hole destruction operator and we have allowed for non-conservation of charge due to the proximity effect. We allow for short-range density-density interactions between the fermions, $\mathcal{H}_{\text{int}} = \dfrac{1}{2}\int dx\,dy\,\rho_{is} V(x-y)\,\rho_{is}$, where the sum over the spin indices is assumed.

Then the effective Hamiltonian, can be derived using a Hartree–Fock (HF) decomposition of the interaction. The charge conserving HF decomposition leads to the interac-

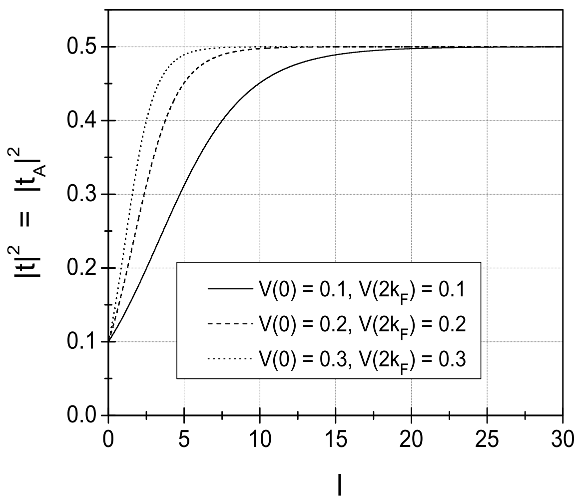

Fig. 2: The variation of $|t|^2$ ($=|t_A|^2$) is plotted as a function of the dimensionless parameter l where $l = ln(L/d)$ and L is either $L_T = \hbar v_F/k_B T$ at zero bias or $L_V = \hbar v_F/eV$ at zero temperature and d is the short distance cut-off for the RG flow. The three curves correspond to three different values of $V(0)$ and $V(2k_F)$ for the NSN junction. This case corresponds to the S-matrix given by S_1.

tion Hamiltonian (normal) of the form

$$\mathcal{H}^N_{\text{int}} = \frac{-i(g_2 - 2g_1)}{4\pi} \int_0^\infty \frac{dx}{x} \Big[r_i^\star \big(\Psi^\dagger_{I\,i\uparrow} \Psi_{O\,i\uparrow} + \Psi^\dagger_{I\,i\downarrow} \Psi_{O\,i\downarrow} \big) - r_i \left(\Psi^\dagger_{O\,i\uparrow} \Psi_{I\,i\uparrow} + \Psi^\dagger_{O\,i\downarrow} \Psi_{I\,i\downarrow} \right) \Big] \tag{2}$$

(We have assumed spin-symmetry and used $r_{i\uparrow} = r_{i\downarrow} = r_i$.) This has been derived earlier in Ref. [7]. We use the same method, but now, we also allow for a charge non-conserving HF decomposition and arrive at the (Andreev) Hamiltonian

$$\mathcal{H}^A_{\text{int}} = \frac{-i(g_1 + g_2)}{4\pi} \int_0^\infty \frac{dx}{x} \Big[- r^\star_{Ai} \big(\Psi^\dagger_{I\,i\uparrow} \Psi^\dagger_{O\,i\downarrow} + \Psi^\dagger_{O\,i\uparrow} \Psi^\dagger_{I\,i\downarrow} \big) + r_{Ai} \left(\Psi_{O\,i\downarrow} \Psi_{I\,i\uparrow} + \Psi_{I\,i\downarrow} \Psi_{O\,i\uparrow} \right) \Big] \tag{3}$$

Note that, even if this appears non-charge conserving, charge conservation is taken care of by the $2e$ charge that flows into the superconductor due to proximity induced Cooper pairing.

In Ref. [7], the perturbatively calculated correction to the reflection amplitude under $\exp[-i\mathcal{H}^N_{\text{int}} t]$ was derived to first order in α. For electrons with spin incident with momentum k with respect to k_F, this was shown to be given by $\frac{-\alpha\, r_i}{2} \ln(kd)$ where $\alpha = (g_2 - 2g_1)/2\pi\hbar v_F$, d is a short distance cutoff and $g_1 = V(2k_F)$, $g_2 = V(0)$. It is worth noting that both g_1 and g_2 scale under RG [6]. Hence, the values given above for g_1 and g_2 are the microscopic values it takes in the original Hamiltonian defined at the short distance scale.

Analogously, here, we calculate the amplitude to go from an incoming electron wave to an outgoing hole wave under $\exp[-i\mathcal{H}^A_{\text{int}} t]$. It is given by $\frac{\alpha'\, r_{A\,i}}{2} \ln(kd)$ where $\alpha' = (g_1 + g_2)/2\pi\hbar v_F$. Note that the spin of the outgoing hole is always the same as the spin of the incoming electron, since the Andreev Hamiltonian also conserves spin for a singlet superconductor. We see that there is a logarithmic singularity at the $k \to 0$ limit which implies that the lowest order perturbation theory is not enough to calculate correction to the reflection and AR amplitudes when the momenta of the incident particles are very close to the Fermi wave vector. Following Yue *et al.* [6], we sum up these most divergent processes using the ”poor man's scaling” approach [15] to obtain RG equations for the normal refection amplitude (r), the transmission amplitude (t), the AR amplitude (r_A), and the CAR amplitude (t_A) which are as follows,

$$\frac{dr}{dl} = -\Big[\frac{\alpha}{2} \left\{ \left(t^2 + r_A^2 + t_A^2 \right) r^\star - r \left(1 - |r|^2 \right) \right\} - \alpha' \left\{ r\, |r_A|^2 + r_A^\star\, t_A\, t \right\} \Big] \tag{4}$$

$$\frac{dr_A}{dl} = -\Big[\alpha \left\{ |r|^2 r_A + t\, t_A\, r^\star \right\} + \frac{\alpha'}{2} \left\{ r_A - \left(r^2 + r_A^2 + t^2 + t_A^2 \right) r_A^\star \right\} \Big] \tag{5}$$

$$\frac{dt}{dl} = -\Big[\alpha \left\{ |r|^2\, t + r^\star\, r_A\, t_A \right\} - \alpha' \left\{ |r_A|^2 t + r\, r_A^\star\, t_A \right\} \Big] \tag{6}$$

$$\frac{dt_A}{dl} = -\Big[\alpha \left\{ r^\star\, r_A\, t + |r|^2\, t_A \right\} - \alpha' \left\{ r\, t\, r_A^\star + |r_A|^2\, t_A \right\} \Big] \tag{7}$$

Note that when $t = t_A = 0$ these equations reduce to the RG equations obtained in Ref. [9] for the case of NS junction.

Results and Discussion. – We propose two possible S-matrices (S_1 and S_2) that can be realized within our set-up which will lead to production of pure SC. The *spin conductance* is defined as $G^S_\uparrow (G^S_\downarrow) \propto |t|^2 + |t_A|^2$ whereas the *charge conductance* is given by $G^C_\uparrow (G^C_\downarrow) \propto -(|t|^2 - |t_A|^2)$. The $\uparrow$ and $\downarrow$ arrows in the subscript represent the spin polarization of the injected electrons from the ferromagnetic lead (see Fig. 1). The negative sign in the expression for $G^C_\uparrow (G^C_\downarrow)$ arises because it is a sum of contribution coming from two oppositely charged particles (electrons and holes). The first S-matrix, S_1 has $r = 0$ (reflection-less), $r_A \neq 0$ and $t = t_A$. This is not a fixed point and hence the parameters of the S-matrix will flow under RG . It is easy

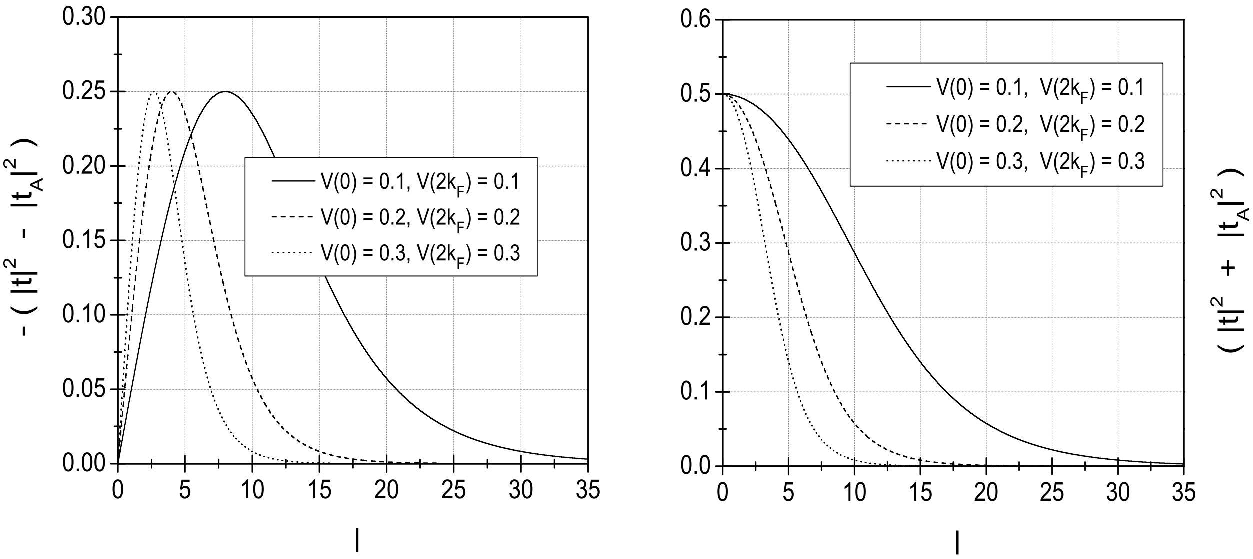

Fig. 3: The variation of $-(|t|^2 - |t_A|^2) \propto G^C_\uparrow$ or $G^C_\downarrow$ and the variation of $(|t|^2 + |t_A|^2) \propto G^S_\uparrow$ or $G^S_\downarrow$ are plotted as a function of the dimensionless parameter l where $l = ln(L/d)$ and L is either $L_T = \hbar v_F/k_B T$ at zero bias or $L_V = \hbar v_F/eV$ at zero temperature and d is the short distance cut-off for the RG flow. The three curves in each plot correspond to three different values of $V(0)$ and $V(2k_F)$ for the NSN junction. These plots correspond to the S-matrix given by S_2.

to see from Eqs. 4 - 7, that for this case, the RG equations for t and t_A are identical, and hence it is ensured that the RG flow will retain the equality of the t and t_A leading to the preservation of pure SC . Physically this implies that if we start the experiment with this given S-matrix (S_1) at the high energy scale (at finite bias voltage and zero temperature *or* at zero bias and finite temperature), then, as we reduce the bias in the zero temperature case (or reduce the temperature in the zero bias case), the correlations arising due to inter-electron interactions in the wire are such that the amplitude of t and t_A will remain equal to each other. The quantity which increases with increasing length scale L is the absolute value of the amplitude t or t_A leading to a monotonic increase of pure SC till it saturates at the maximum value allowed by the symmetries of the S-matrix, S_1 (Fig. 2). Here all the S-matrix elements are assumed to be energy independent and hence the bias dependence is solely due to RG flow. Of course the bias window has to be small enough so that the energy dependence of t, t_A, r and r_A can be safely ignored. This saturation point is actually a stable fixed point of the theory if the junction remains reflection-less. So we observe that the transmission (both t and t_A) increases to maximum value while the AR amplitude scales down to zero. This flow direction is quite different from that of the standard case of a single impurity in an interacting electron gas in 1–D where any small but finite reflection amplitude gets enhanced under RG flow ultimately leading to zero transmission [16]. The difference here is because the RG flow is solely due to the existence of the finite pair potential (due to r_A) and not due to the usual Friedel oscillations (due to r). Hence the electrons in the wire have an effective attractive interaction leading to a counter intuitive RG flow. We remark that the interaction induced correction enhances the amplitude for pure SC and also stabilizes the pure SC operating point. This makes the operating point, S_1 quite well-suited for an experimental situation. Fig. 2 shows the variation of the pure spin conductance ($= 2 \times |t|^2$ in units of e^2/h) as a function of relevant length scale, L of the problem.

The second case corresponds to the most symmetric S-matrix (S_2). It is a fixed point of RG equations and is given by $r = 1/2, r_A = -1/2, t = 1/2, t_A = 1/2$. Here also t is equal to t_A as in the previous case and thus the junction will act like a perfect charge filter resulting in pure SC in the right wire (if spin polarized charge current is injected in the left wire). However, this S-matrix (S_2) represents an unstable fixed point. Due to any small perturbation, the parameters tend to flow away from this unstable fixed point to the most stable disconnected fixed point given by $|r| = 1$ as a result of RG flow. So this S-matrix (S_2) is not a stable operating point for the production of pure SC. But, it is interesting to note that if we switch on a small perturbation around this fixed point, the charge conductance exhibits a non-monotonic behavior under RG flow (Fig. 3). This non-monotonicity results from two competing effects *viz.*, transport through both electron and hole channels and, the RG flow of g_1, g_2. This essentially leads to negative differential conductance (NDC) [17]. Elaborating it further, all it means is that if we start an experiment

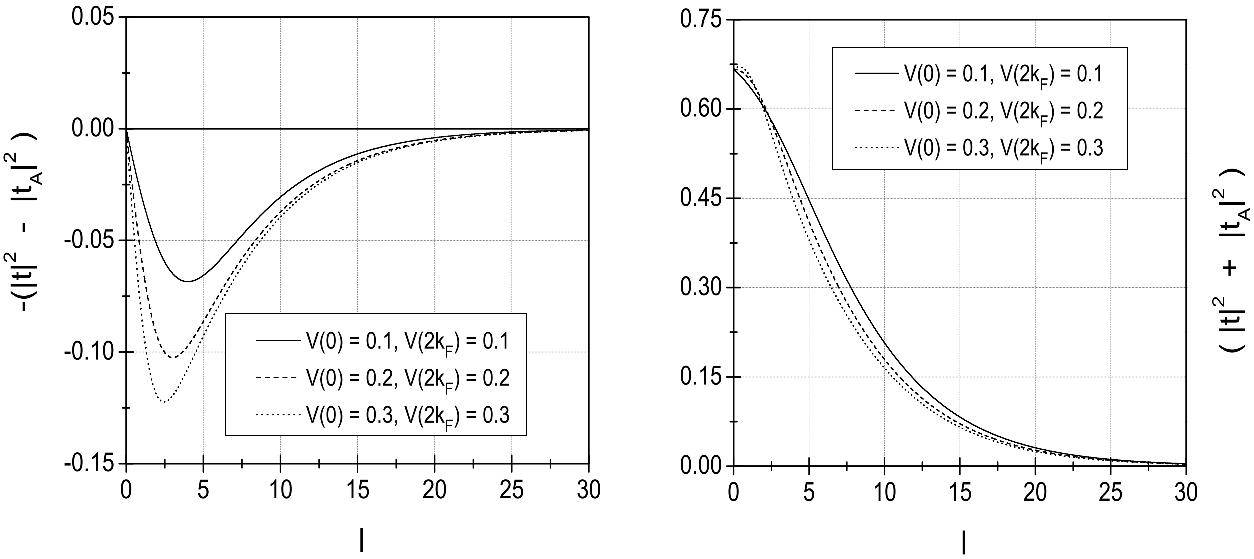

Fig. 4: The variation of $-(|t|^2 - |t_A|^2) \propto G^C_\uparrow$ or $G^C_\downarrow$ and the variation of $(|t|^2 + |t_A|^2) \propto G^S_\uparrow$ or $G^S_\downarrow$ are plotted in left and right panel plots as a function of the dimensionless parameter l where $l = ln(L/d)$ and L is either $L_T = \hbar v_F / k_B T$ at zero bias or $L_V = \hbar v_F / eV$ at zero temperature and d is the short distance cut-off for the RG flow. The three curves in each plot correspond to three different values of $V(0)$ and $V(2k_F)$ for the FSN junction. These plots correspond to the S-matrix given by S_3.

with this given S-matrix (S_2) at zero temperature and at finite bias, then as we go towards zero bias,the conductance will show a rise with decreasing bias for a certain bias window. This can be seen from Fig. 3. This aspect of the RG flow can be of direct relevance for manipulating electron and spin transport in some mesoscopic devices.

Now we will switch to the case of ferromagnetic half metal−superconductor−normal metal (FSN) junction which comprises of a 1–D ferromagnetic half metal (assuming $\uparrow$ polarization) on one side and a normal 1–D metal on the other side (in a way similar to the set-up shown in Fig. 1). This case is very complicated to study theoretically because the minimal number of independent complex-valued parameters that are required to parameterize the S-matrix is nine as opposed to the previous (symmetric) case which had only four such parameters. These are given by $r^{11}_{\uparrow\uparrow}$, $r^{22}_{\uparrow\uparrow}$, $r^{22}_{\downarrow\downarrow}$, $t^{12}_{A\uparrow\uparrow}$, $t^{21}_{A\downarrow\downarrow}$, $r^{22}_{A\uparrow\uparrow}$, $r^{22}_{A\downarrow\downarrow}$, $t^{12}_{\uparrow\uparrow}$, and $t^{21}_{\uparrow\uparrow}$. Here, 1(2) is the wire index for the ferromagnetic (normal) wire while, $\uparrow$ and $\downarrow$ are the respective spin polarization indices for the electron. The large number of independent parameters in this case arise because of the presence of ferromagnetic half-metallic wire which destroys both the spin rotation symmetry and the left-right symmetry. The only remaining symmetry is the particle-hole symmetry. Analogous to the RG equations (given by Eqs. 4-7) for the NSN case, it is possible to write down all the nine RG equations for FSN case and solve them numerically to obtain the results as shown in Fig. 4. (For further details, see Ref. [18]). In this case, the elements of a representative S-matrix (S_3) which correspond to the production of pure SC are $|r^{11}_{\uparrow\uparrow}| = |r^{22}_{\uparrow\uparrow}| = |r^{22}_{\downarrow\downarrow}| = |t^{12}_{A\uparrow\uparrow}| = |t^{21}_{A\downarrow\downarrow}| = |r^{22}_{A\uparrow\uparrow}| = |r^{22}_{A\downarrow\downarrow}| = |t^{12}_{\uparrow\uparrow}| = |t^{21}_{\uparrow\uparrow}| = 1/\sqrt{3}$ and the corresponding phases associated with each of these amplitudes are $\pi/3, \pi, 0, -\pi/3, 0, \pi/3, 0, \pi, -\pi/3$ respectively. By solving the nine coupled RG equations for the above mentioned nine independent parameters, we have checked numerically that this is *not* a fixed point of the RG equation and hence it will flow under RG and finally reach the trivial stable fixed point given by $r^{11}_{\uparrow\uparrow} = r^{22}_{\uparrow\uparrow} = r^{22}_{\downarrow\downarrow} = 1$. Now if we impose a bias on the system from left to right, it will create a pure SC on the right wire because $|t^{12}_{A\uparrow\uparrow}|$ is exactly equal to $|t^{12}_{\uparrow\uparrow}|$. But of course, this is a highly unstable operating point for production of pure SC as this is not even a fixed point and hence will always flow under any variation of temperature or bias destroying the production of pure SC. In this case also, the spin conductance shows a monotonic behavior while, the charge conductance is non-monotonic and hence will have NDC in some parameter regime. It is worth noticing that in this case the interaction parameters g_1 and g_2 both do not scale on the left wire as it is completely spin polarized while g_1 and g_2 do scale on the right wire as it is not spin polarized. Hence even if we begin our RG flow with symmetric interaction strengths on both left and right wires, they will develop an asymmetry under the RG flow.

Finally, we consider another important aspect that nicely characterizes these hybrid structures from a spintronics application point of view. If the QW on the two sides of the superconductor are ferromagnetic half metals then we have a junction of ferromagnet−superconductor−ferromagnet (FSF). We calculate the tunnelling magnetoresistance ratio (TMR) [2] which is defined as follows

$$\mathsf{TMR} = \left[\frac{G_{\uparrow\uparrow} - G_{\uparrow\downarrow}}{G_{\uparrow\downarrow}}\right] \tag{8}$$

Here, $G_{\uparrow\uparrow}$ corresponds to the conductance across the junction when both left and right wires are in parallel spin-polarized configurations. $G_{\uparrow\downarrow}$ corresponds to the case when the left and right wires are in anti-parallel spin-polarized configurations. Thus, TMR is the maximum relative change in resistance in going from the parallel to the anti-parallel configuration. For the parallel case, the CAR amplitude (t_A) is zero and the only process which contributes to the conductance is the direct tunnelling process. This is because the CAR process involves non-local pairing of $\uparrow$ e in the left wire with $\downarrow$ e in the right wire to form a Cooper pair. However for $\downarrow$ e , the density of states is zero in the right wire which makes this process completely forbidden. Hence, $G_{\uparrow\uparrow} \propto |t|^2$. On the other hand, for the anti-parallel case, $G_{\uparrow\downarrow} \propto -|t_A|^2$ as there is no density of states for the $\uparrow$ e in the right lead and so no direct tunnelling of $\uparrow$ e across the junction is allowed; hence CAR is the only allowed process. Note that the negative sign in $G_{\uparrow\downarrow}$ leads to a very large enhancement of TMR (as opposed to the case of standard ferromagnet−normal metal−ferromagnet (FNF) junction) since the two contributions will add up. A related set-up has been studied in [19] where also a large TMR has been obtained.

One can then do the RG analysis for both parallel and anti-parallel cases. It turns out that the equations for $|t|$ and $|t_A|$ are identical leading to identical temperature (bias) dependance. The RG equation for $|t_A|$ is

$$\frac{dt_A}{dl} = -\beta\, t_A \left[1 - |t_A|^2\right] \tag{9}$$

Here, $\beta = (g_2 - g_1)/2\pi\hbar v_F$. $|t|$ satisfies the same equation. So, in a situation where the reflection amplitudes at the junction for the two cases are taken to be equal then it follows from Eq. 8 that the TMR will be pinned to its maximum value *i.e.* magnitude of TMR $= 2$ and the temperature dependence will be flat even in the presence of inter-electron interactions.

Conclusions. – In this letter, we have studied both spin and charge transport in NSN, FSN, and FSF structures in the context of 1–D QW. We calculated the corrections to spin and charge transport arising from inter-electron interactions in the QW. We demonstrated the possibility for production of pure SC in such hybrid junctions and analysed its stability against temperature and voltage variations. Finally, we also showed that the presence of the CAR process heavily enhances the TMR in such geometries.

We acknowledge use of the Beowulf cluster at H.R.I. S.D. was supported by the Feinberg Fellowship Programme at WIS, Israel.

REFERENCES

[1] Datta S. and Das B., *Appl. Phys. Lett.* , **56** (1990) 665.
[2] Zutik I., Fabian J. and Sharma S. D., *Reviews of Modern Physics* , **76** (2004) 323.
[3] Rashba E. I., *Physica E* , **34** (2006) 31.
[4] Watson S. K., Potok R. M., Marcus C. M. and Umansky V., *Phys. Rev. Lett.* , **91** (2003) 258301.
[5] Bignon G., Houzet M., Pistolesi F. and Hekking F. W. J., *Europhys. Lett.* , **67** (2004) 110.
[6] Yue D., Glazman L. I. and Matveev K. A., *Phys. Rev. B* , **49** (1994) 1966.
[7] Lal S., Rao S. and Sen D., *Phys. Rev. B* , **66** (2002) 165327.
[8] Das S., Rao S. and Sen D., *Phys. Rev. B* , **70** (2004) 085318.
[9] Takane T. and Koyama Y., *J. Phys. Soc. Jpn.* , **66** (1997) 419.
[10] Man H. T., Klapwijk T. M. and Morpurgo A. F., *Transport through a superconductor-interacting normal metal junction: a phenomenological description*, `cond-mat/0504566` (2005).
[11] Titov M., Müller M. and Belzig W., *Physical Review Letters* , **97** (2006) 237006.
[12] Takane T. and Koyama Y., *J. Phys. Soc. Jpn.* , **65** (1996) 3630.
[13] Fazio R., Hekking F. W. J., Odintsov A. A. and Raimondi R., *Superlattices Microstruct.* , **25** (1999) 1163.
[14] C. Winkelholz, Rosario Fazio F. W. H. and Schn G., *Phys. Rev. Lett.* , **77** (1996) 3200.
[15] Anderson P. W., *Journal of Physics C: Solid State Physics* , **3** (1970) 2436.
[16] Kane C. L. and Fisher M. P. A., *Phys. Rev. B* , **46** (1992) 15233.
[17] Esaki L., *Phys. Rev.* , **109** (1958) 603.
[18] Das S., Rao S. and Saha A., manuscript under preparation.
[19] Francesco Giazotto, Fabio Taddei F. B. and Fazio R., *Phys. Rev. Lett.* , **97** (2006) 087001.

Spintronics with NSN Junction of one-dimensional quantum wires: A study of Pure Spin Current and Magnetoresistance

Sourin Das[1], Sumathi Rao[2] and Arijit Saha[2]

[1] *Department of Condensed Matter Physics, Weizmann Institute of Science, Rehovot 76 100, Israel*
[2] *Harish−Chandra Research Institute, Chhatnag Road, Jhusi, Allahabad 211 019, India*

PACS 73.23.-b – Electronic transport in mesoscopic systems
PACS 74.45.+c – Proximity effects; Andreev effect; SN and SNS junctions
PACS 72.25.Ba – Spin polarized transport in metals

Abstract. - We demonstrate possible scenarios for production of pure spin current and large tunnelling magnetoresistance ratios from elastic co-tunnelling and crossed Andreev reflection across a superconducting junction comprising of normal metal-superconductor-normal metal, where, the normal metal is a one-dimensional interacting quantum wire. We show that there are fixed points in the theory which correspond to the case of pure spin current. We analyze the influence of electron-electron interaction and see how it stabilizes or de-stabilizes the production of pure spin current. These fixed points can be of direct experimental relevance for spintronics application of normal metal-superconductor-normal metal junctions of one-dimensional quantum wires. We also calculate the power law temperature dependence of the crossed Andreev reflection enhanced tunnelling magnetoresistance ratio for the normal metal-superconductor-normal metal junction.

Introduction. – Two fundamental degrees of freedom associated with an electron that are of direct interest to condensed matter physics are its charge and spin. Until very recently, all conventional electron-based devices have been solely based upon the utilization and manipulation of the charge degree of freedom of an electron. However, the realization of the fact that devices based on the spin degree of freedom can be almost dissipation-less and with very fast switching times, has led to an upsurge in research activity in this direction in recent years [?, ?, ?]. The first step towards realization of spin-based electronics (spintronics) would be to produce pure spin current (SC). From a purely theoretical point of view, it is straight forward to define a charge current as a product of local charge density with the charge velocity, but such a definition cannot be straight forwardly extended to the case of SC. This is because both spin $\vec{S}$ and velocity $\vec{v}$ are vector quantities and hence the product of two such vectors will be a tensor.

In this letter, we adopt the simple minded definition of SC, which is commonly used [?]. It is just the product of the local spin polarization density associated with the electron or hole, (a scalar s which is either positive for up-spin or negative for down-spin) and its velocity [?]. The most obvious scenario in which one can generate a pure SC in the sense defined above would be to have *(a)* an equal and opposite flow of identically spin-polarized electrons through a channel, such that the net charge current through the channel is nullified leaving behind a pure SC, or *(b)* alternatively, an equal flow of identically spin polarized electrons and holes in the same direction through a channel giving rise to pure SC with perfect cancellation of charge current. In this letter, we explore the second possibility for generating pure SC using a normal metal−superconductor−normal metal (NSN) junction.

Proposed device and its theoretical modelling. – The configuration we have in mind for the production of pure SC is shown in Fig. 1. The idea is to induce a pair potential in a small region of a quantum wire (QW) by depositing a superconducting strip on top of the wire (which may be, for instance, a carbon nanotube) due to proximity effects. If the strip width on the wire is of the order of the phase coherence length of the superconductor, then both direct electron to electron co-tunnelling as well as crossed Andreev electron to hole tunnelling can occur across the superconducting region [?]. It is worth pointing out that in the case of a singlet superconductor, which is the case we consider, both the tunnelling processes will conserve spin. In order to describe the mode of operation of the device (see Fig. 1), we first assume that the S-matrix rep-

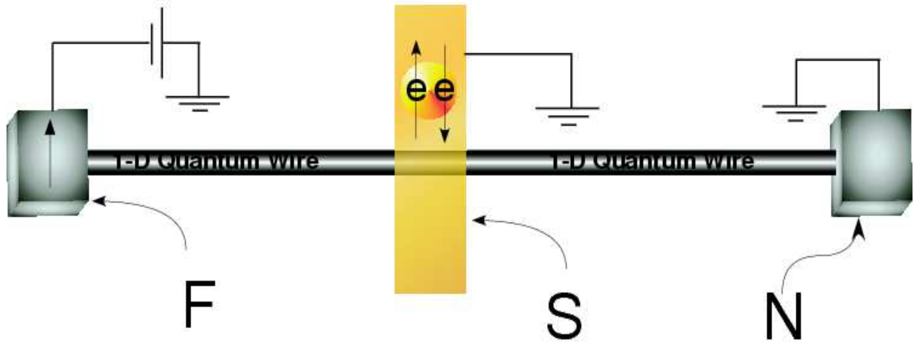

Fig. 1: A 1–D quantum wire (carbon nanotube) connected to a ferromagnetic (F) lead on the left and a normal (N) lead on the right. The thin strip in the middle of the wire depicts a 2–D layer of superconducting material deposited on top of the wire.

resenting the NSN junction described above respects parity symmetry about the junction, particle-hole symmetry and spin-rotation symmetry. Considering all the symmetries, we can describe the superconducting junction connecting the two half wires by an S-matrix with only four independent parameters namely, *(i)* the normal refection amplitude (r) for e (h), *(ii)* the transmission amplitude (t) for e (h), *(iii)* the Andreev reflection (AR) amplitude (r_A) for e (h), and *(iv)* the crossed Andreev reflection (CAR) amplitude (t_A) for e (h). If we inject spin polarized electron ($\uparrow$ e) from the left QW using a ferromagnetic contact and tune the junction parameters such that t and t_a are equal to each other, it will lead to a pure SC flowing in the right QW (see Fig. 1). This is so because, on an average, an equal number of electrons ($\uparrow$ e) (direct electron to electron tunnelling) and holes ($\uparrow$ h) (crossed Andreev electron to hole tunnelling) are injected from the left wire to the right wire resulting in production of pure SC in the right wire. Note that spin up holes ($\uparrow$ h) implies a Fermi sea with an absence of spin down electron (which is what is needed for the incident electron ($\uparrow$ e) to form a Cooper pair and enter the singlet superconductor).

Renormalisation Group study. – We now include the effects of inter-electron interactions on the S-matrix using the renormalisation group (RG) method introduced in Ref. [?]. This was furthur generalized to the case of multiple wires in Refs. [?, ?] and to the case of 1–D NS junction [?, ?, ?]. The basic idea of the method is as follows. The presence of scattering (reflection) induces Friedel oscillations in the density of non-interacting electrons. Within a mean field picture for a weakly interacting electron gas, the electron not only scatters off the potential barrier but also scatters off these density oscillations with an amplitude proportional to the interaction strength. Hence by calculating the total reflection amplitude due to scattering from the scalar potential scatterer and from the Friedel oscillations created by the scatterer, we can include the effect of electron-electron interaction in calculating transport. This approach can be generalized to junctions of one-dimensional (1–D) QW with a single superconductor. In this case, there will be non-zero AR in the bulk of the wire due to proximity induced pair potential, besides the AR right at the NSN junction which turns an incoming electron into an outgoing hole.

The RG equations for a NS case have been obtained earlier using bosonization [?,?,?] and using WIRG [?,?]. In this letter we extend these WIRG results to the NSN case. To obtain the RG equations in the presence of AR and CAR for the NSN junction, we follow a procedure similar to that used in Ref. [?]. The fermion fields expanded around the left and right Fermi momenta on each wire can be written as, $\psi_{is}(x) = \Psi_{I\,is}(x)\,e^{i\,k_F\,x} + \Psi_{O\,is}(x)\,e^{-i\,k_F\,x}$; where i is the wire index, s is the spin index which can be $\uparrow,\downarrow$ and $I(O)$ stand for incoming (outgoing) fields. Note that $\Psi_{I(O)}(x)$ are slowly varying fields on the scale of k_F^{-1}. For a momentum in the vicinity of k_F, the incoming and outgoing fields can be Fourier expanded as:

$$
\begin{aligned}
\Psi_{ks}(x) \;&=\; \int dk\,\Big[b_{ks}\,e^{i\,(k+k_F)\,x} + d^{\dagger}_{ks}\,e^{i\,(-k+k_F)\,x} \\
&\quad + r\,b_{ks}\,e^{-i\,(k+k_F)\,x} + r^{\star}\,d^{\dagger}_{ks}\,e^{-i\,(-k+k_F)\,x} \\
&\quad + r_A\,d_{ks}\,e^{-i\,(-k+k_F)\,x} + r^{\star}_A\,b^{\dagger}_{ks}\,e^{-i\,(k+k_F)\,x}\Big]
\end{aligned} \tag{1}
$$

where b_{ks} is the electron destruction operator and d_{ks} is the hole destruction operator and we have allowed for non-conservation of charge due to the proximity effect. We allow for short-range density-density interactions between the fermions, $\mathcal{H}_{\mathsf{int}} = \dfrac{1}{2}\int dx\,dy\,\rho_{is}V(x-y)\,\rho_{is}$, where the sum over the spin indices is assumed.

Then the effective Hamiltonian, can be derived using a Hartree−Fock (HF) decomposition of the interaction. The charge conserving HF decomposition leads to the interac-

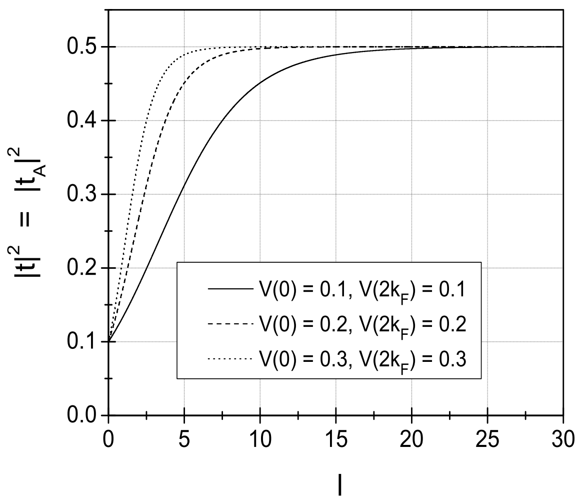

Fig. 2: The variation of $|t|^2$ ($=|t_A|^2$) is plotted as a function of the dimensionless parameter l where $l = ln(L/d)$ and L is either $L_T = \hbar v_F/k_BT$ at zero bias or $L_V = \hbar v_F/eV$ at zero temperature and d is the short distance cut-off for the RG flow. The three curves correspond to three different values of $V(0)$ and $V(2k_F)$ for the NSN junction. This case corresponds to the S-matrix given by S_1.

tion Hamiltonian (normal) of the form

$$\mathcal{H}^N_{\text{int}} = \frac{-i(g_2-2g_1)}{4\pi}\int_0^\infty \frac{dx}{x}\Big[r_i^\star(\Psi^\dagger_{I\,i\uparrow}\Psi_{O\,i\uparrow} + \Psi^\dagger_{I\,i\downarrow}\Psi_{O\,i\downarrow}) - r_i\left(\Psi^\dagger_{O\,i\uparrow}\Psi_{I\,i\uparrow} + \Psi^\dagger_{O\,i\downarrow}\Psi_{I\,i\downarrow}\right)\Big] \quad (2)$$

(We have assumed spin-symmetry and used $r_{i\uparrow} = r_{i\downarrow} = r_i$.) This has been derived earlier in Ref. [?]. We use the same method, but now, we also allow for a charge non-conserving HF decomposition and arrive at the (Andreev) Hamiltonian

$$\mathcal{H}^A_{\text{int}} = \frac{-i(g_1+g_2)}{4\pi}\int_0^\infty \frac{dx}{x}\Big[-r^\star_{Ai}(\Psi^\dagger_{I\,i\uparrow}\Psi^\dagger_{O\,i\downarrow} + \Psi^\dagger_{O\,i\uparrow}\Psi^\dagger_{I\,i\downarrow}) + r_{Ai}\left(\Psi_{O\,i\downarrow}\Psi_{I\,i\uparrow} + \Psi_{I\,i\downarrow}\Psi_{O\,i\uparrow}\right)\Big] \quad (3)$$

Note that, even if this appears non-charge conserving, charge conservation is taken care of by the $2e$ charge that flows into the superconductor due to proximity induced Cooper pairing.

In Ref. [?], the perturbatively calculated correction to the reflection amplitude under $\exp[-i\mathcal{H}^N_{\text{int}}t]$ was derived to first order in α. For electrons with spin incident with momentum k with respect to k_F, this was shown to be given by $\dfrac{-\alpha\, r_i}{2}\ln(kd)$ where $\alpha = (g_2 - 2g_1)/2\pi\hbar v_F$, d is a short distance cutoff and $g_1 = V(2k_F)$, $g_2 = V(0)$. It is worth noting that both g_1 and g_2 scale under RG [?]. Hence, the values given above for g_1 and g_2 are the microscopic values it takes in the original Hamiltonian defined at the short distance scale.

Analogously, here, we calculate the amplitude to go from an incoming electron wave to an outgoing hole wave under $\exp[-i\mathcal{H}^A_{\text{int}}t]$. It is given by $\dfrac{\alpha'\, r_{A\,i}}{2}\ln(kd)$ where $\alpha' = (g_1+g_2)/2\pi\hbar v_F$. Note that the spin of the outgoing hole is always the same as the spin of the incoming electron, since the Andreev Hamiltonian also conserves spin for a singlet superconductor. We see that there is a logarithmic singularity at the $k \to 0$ limit which implies that the lowest order perturbation theory is not enough to calculate correction to the reflection and AR amplitudes when the momenta of the incident particles are very close to the Fermi wave vector. Following Yue *et al.* [?], we sum up these most divergent processes using the "poor man's scaling" approach [?] to obtain RG equations for the normal refection amplitude (r), the transmission amplitude (t), the AR amplitude (r_A), and the CAR amplitude (t_A) which are as follows,

$$\frac{dr}{dl} = -\Big[\frac{\alpha}{2}\left\{\left(t^2 + r_A^2 + t_A^2\right)r^\star - r\left(1-|r|^2\right)\right\} - \alpha'\left\{r\,|r_A|^2 + r_A^\star\, t_A\, t\right\}\Big] \quad (4)$$

$$\frac{dr_A}{dl} = -\Big[\alpha\left\{|r|^2 r_A + t\,t_A\,r^\star\right\} + \frac{\alpha'}{2}\left\{r_A - \left(r^2 + r_A^2 + t^2 + t_A^2\right)r_A^\star\right\}\Big] \quad (5)$$

$$\frac{dt}{dl} = -\Big[\alpha\left\{|r|^2\,t + r^\star\,r_A\,t_A\right\} - \alpha'\left\{|r_A|^2 t + r\,r_A^\star\,t_A\right\}\Big] \quad (6)$$

$$\frac{dt_A}{dl} = -\Big[\alpha\left\{r^\star\,r_A\,t + |r|^2\,t_A\right\} - \alpha'\left\{r\,t\,r_A^\star + |r_A|^2\,t_A\right\}\Big] \quad (7)$$

Note that when $t = t_A = 0$ these equations reduce to the RG equations obtained in Ref. [?] for the case of NS junction.

Results and Discussion. – We propose two possible S-matrices (S_1 and S_2) that can be realized within our set-up which will lead to production of pure SC. The *spin conductance* is defined as $G^S_\uparrow(G^S_\downarrow) \propto |t|^2 + |t_A|^2$ whereas the *charge conductance* is given by $G^C_\uparrow(G^C_\downarrow) \propto -(|t|^2 - |t_A|^2)$. The $\uparrow$ and $\downarrow$ arrows in the subscript represent the spin polarization of the injected electrons from the ferromagnetic lead (see Fig. 1). The negative sign in the expression for $G^C_\uparrow(G^C_\downarrow)$ arises because it is a sum of contribution coming from two oppositely charged particles (electrons and holes). The first S-matrix, S_1 has $r = 0$ (reflection-less), $r_A \neq 0$ and $t = t_A$. This is not a fixed point and hence the parameters of the S-matrix will flow under RG . It is easy

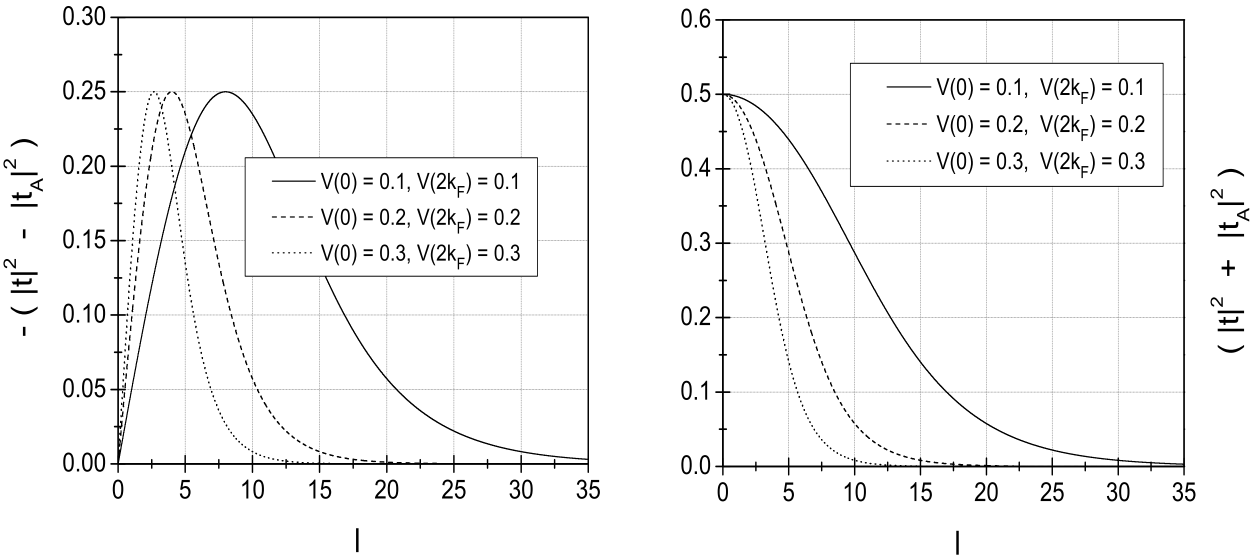

Fig. 3: The variation of $-(|t|^2 - |t_A|^2) \propto G^C_\uparrow$ or $G^C_\downarrow$ and the variation of $(|t|^2 + |t_A|^2) \propto G^S_\uparrow$ or $G^S_\downarrow$ are plotted as a function of the dimensionless parameter l where $l = ln(L/d)$ and L is either $L_T = \hbar v_F/k_BT$ at zero bias or $L_V = \hbar v_F/eV$ at zero temperature and d is the short distance cut-off for the RG flow. The three curves in each plot correspond to three different values of $V(0)$ and $V(2k_F)$ for the NSN junction. These plots correspond to the S-matrix given by S_2.

to see from Eqs. 4 - 7, that for this case, the RG equations for t and t_A are identical, and hence it is ensured that the RG flow will retain the equality of the t and t_A leading to the preservation of pure SC . Physically this implies that if we start the experiment with this given S-matrix (S_1) at the high energy scale (at finite bias voltage and zero temperature *or* at zero bias and finite temperature), then, as we reduce the bias in the zero temperature case (or reduce the temperature in the zero bias case), the correlations arising due to inter-electron interactions in the wire are such that the amplitude of t and t_A will remain equal to each other. The quantity which increases with increasing length scale L is the absolute value of the amplitude t or t_A leading to a monotonic increase of pure SC till it saturates at the maximum value allowed by the symmetries of the S-matrix, S_1 (Fig. 2). Here all the S-matrix elements are assumed to be energy independent and hence the bias dependence is solely due to RG flow. Of course the bias window has to be small enough so that the energy dependence of t, t_A, r and r_A can be safely ignored. This saturation point is actually a stable fixed point of the theory if the junction remains reflection-less. So we observe that the transmission (both t and t_A) increases to maximum value while the AR amplitude scales down to zero. This flow direction is quite different from that of the standard case of a single impurity in an interacting electron gas in 1–D where any small but finite reflection amplitude gets enhanced under RG flow ultimately leading to zero transmission [?]. The difference here is because the RG flow is solely due to the existence of the finite pair potential (due to r_A) and not due to the usual Friedel oscillations (due to r). Hence the electrons in the wire have an effective attractive interaction leading to a counter intuitive RG flow. We remark that the interaction induced correction enhances the amplitude for pure SC and also stabilizes the pure SC operating point. This makes the operating point, S_1 quite well-suited for an experimental situation. Fig. 2 shows the variation of the pure spin conductance ($= 2 \times |t|^2$ in units of e^2/h) as a function of relevant length scale, L of the problem.

The second case corresponds to the most symmetric S-matrix (S_2). It is a fixed point of RG equations and is given by $r = 1/2, r_A = -1/2, t = 1/2, t_A = 1/2$. Here also t is equal to t_A as in the previous case and thus the junction will act like a perfect charge filter resulting in pure SC in the right wire (if spin polarized charge current is injected in the left wire). However, this S-matrix (S_2) represents an unstable fixed point. Due to any small perturbation, the parameters tend to flow away from this unstable fixed point to the most stable disconnected fixed point given by $|r| = 1$ as a result of RG flow. So this S-matrix (S_2) is not a stable operating point for the production of pure SC. But, it is interesting to note that if we switch on a small perturbation around this fixed point, the charge conductance exhibits a non-monotonic behavior under RG flow (Fig. 3). This non-monotonicity results from two competing effects *viz.*, transport through both electron and hole channels and, the RG flow of g_1, g_2. This essentially leads to negative differential conductance (NDC) [?]. Elaborating it further, all it means is that if we start an experiment

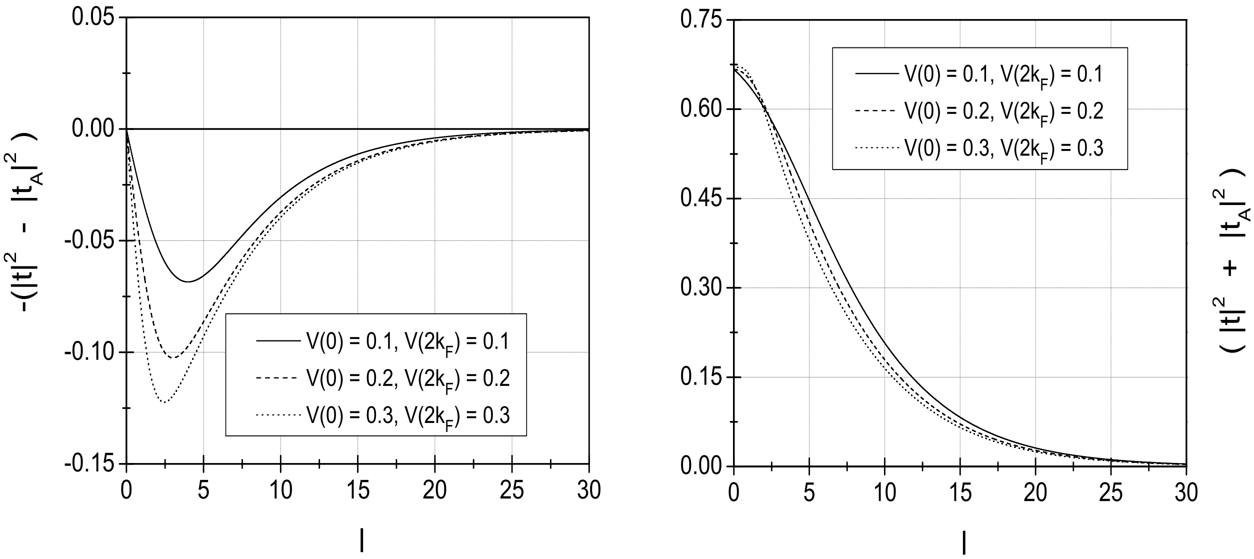

Fig. 4: The variation of $-(|t|^2 - |t_A|^2) \propto G^C_\uparrow$ or $G^C_\downarrow$ and the variation of $(|t|^2 + |t_A|^2) \propto G^S_\uparrow$ or $G^S_\downarrow$ are plotted in left and right panel plots as a function of the dimensionless parameter l where $l = ln(L/d)$ and L is either $L_T = \hbar v_F/k_B T$ at zero bias or $L_V = \hbar v_F/eV$ at zero temperature and d is the short distance cut-off for the RG flow. The three curves in each plot correspond to three different values of $V(0)$ and $V(2k_F)$ for the FSN junction. These plots correspond to the S-matrix given by S_3.

with this given S-matrix (S_2) at zero temperature and at finite bias, then as we go towards zero bias,the conductance will show a rise with decreasing bias for a certain bias window. This can be seen from Fig. 3. This aspect of the RG flow can be of direct relevance for manipulating electron and spin transport in some mesoscopic devices.

Now we will switch to the case of ferromagnetic half metal−superconductor−normal metal (FSN) junction which comprises of a 1–D ferromagnetic half metal (assuming $\uparrow$ polarization) on one side and a normal 1–D metal on the other side (in a way similar to the set-up shown in Fig. 1). This case is very complicated to study theoretically because the minimal number of independent complex-valued parameters that are required to parameterize the S-matrix is nine as opposed to the previous (symmetric) case which had only four such parameters. These are given by $r^{11}_{\uparrow\uparrow}$, $r^{22}_{\uparrow\uparrow}$, $r^{22}_{\downarrow\downarrow}$, $t^{12}_{A\uparrow\uparrow}$, $t^{21}_{A\downarrow\downarrow}$, $r^{22}_{A\uparrow\uparrow}$, $r^{22}_{A\downarrow\downarrow}$, $t^{12}_{\uparrow\uparrow}$, and $t^{21}_{\uparrow\uparrow}$. Here, 1(2) is the wire index for the ferromagnetic (normal) wire while, $\uparrow$ and $\downarrow$ are the respective spin polarization indices for the electron. The large number of independent parameters in this case arise because of the presence of ferromagnetic half-metallic wire which destroys both the spin rotation symmetry and the left-right symmetry. The only remaining symmetry is the particle-hole symmetry. Analogous to the RG equations (given by Eqs. 4-7) for the NSN case, it is possible to write down all the nine RG equations for FSN case and solve them numerically to obtain the results as shown in Fig. 4. (For further details, see Ref. [?]). In this case, the elements of a representative S-matrix (S_3) which correspond to the production of pure SC are $|r^{11}_{\uparrow\uparrow}| = |r^{22}_{\uparrow\uparrow}| = |r^{22}_{\downarrow\downarrow}| = |t^{12}_{A\uparrow\uparrow}| = |t^{21}_{A\downarrow\downarrow}| = |r^{22}_{A\uparrow\uparrow}| = |r^{22}_{A\downarrow\downarrow}| = |t^{12}_{\uparrow\uparrow}| = |t^{21}_{\uparrow\uparrow}| = 1/\sqrt{3}$ and the corresponding phases associated with each of these amplitudes are $\pi/3, \pi, 0, -\pi/3, 0, \pi/3, 0, \pi, -\pi/3$ respectively. By solving the nine coupled RG equations for the above mentioned nine independent parameters, we have checked numerically that this is *not* a fixed point of the RG equation and hence it will flow under RG and finally reach the trivial stable fixed point given by $r^{11}_{\uparrow\uparrow} = r^{22}_{\uparrow\uparrow} = r^{22}_{\downarrow\downarrow} = 1$. Now if we impose a bias on the system from left to right, it will create a pure SC on the right wire because $|t^{12}_{A\uparrow\uparrow}|$ is exactly equal to $|t^{12}_{\uparrow\uparrow}|$. But of course, this is a highly unstable operating point for production of pure SC as this is not even a fixed point and hence will always flow under any variation of temperature or bias destroying the production of pure SC. In this case also, the spin conductance shows a monotonic behavior while, the charge conductance is non-monotonic and hence will have NDC in some parameter regime. It is worth noticing that in this case the interaction parameters g_1 and g_2 both do not scale on the left wire as it is completely spin polarized while g_1 and g_2 do scale on the right wire as it is not spin polarized. Hence even if we begin our RG flow with symmetric interaction strengths on both left and right wires, they will develop an asymmetry under the RG flow.

Finally, we consider another important aspect that nicely characterizes these hybrid structures from a spintronics application point of view. If the QW on the two sides of the superconductor are ferromagnetic half metals then we have a junction of ferromagnet−superconductor−ferromagnet (FSF). We calculate the tunnelling magnetoresistance ratio (TMR) [?] which is defined as follows

$$\mathsf{TMR} = \left[\frac{G_{\uparrow\uparrow} - G_{\uparrow\downarrow}}{G_{\uparrow\downarrow}}\right] \tag{8}$$

Here, $G_{\uparrow\uparrow}$ corresponds to the conductance across the junction when both left and right wires are in parallel spin-polarized configurations. $G_{\uparrow\downarrow}$ corresponds to the case when the left and right wires are in anti-parallel spin-polarized configurations. Thus, TMR is the maximum relative change in resistance in going from the parallel to the anti-parallel configuration. For the parallel case, the CAR amplitude (t_A) is zero and the only process which contributes to the conductance is the direct tunnelling process. This is because the CAR process involves non-local pairing of $\uparrow$ e in the left wire with $\downarrow$ e in the right wire to form a Cooper pair. However for $\downarrow$ e , the density of states is zero in the right wire which makes this process completely forbidden. Hence, $G_{\uparrow\uparrow} \propto |t|^2$. On the other hand, for the anti-parallel case, $G_{\uparrow\downarrow} \propto -|t_A|^2$ as there is no density of states for the $\uparrow$ e in the right lead and so no direct tunnelling of $\uparrow$ e across the junction is allowed; hence CAR is the only allowed process. Note that the negative sign in $G_{\uparrow\downarrow}$ leads to a very large enhancement of TMR (as opposed to the case of standard ferromagnet−normal metal−ferromagnet (FNF) junction) since the two contributions will add up. A related set-up has been studied in [**?**] where also a large TMR has been obtained.

One can then do the RG analysis for both parallel and anti-parallel cases. It turns out that the equations for $|t|$ and $|t_A|$ are identical leading to identical temperature (bias) dependance. The RG equation for $|t_A|$ is

$$\frac{dt_A}{dl} = -\beta\, t_A\, \left[1 - |t_A|^2\right] \tag{9}$$

Here, $\beta = (g_2 - g_1)/2\pi\hbar v_F$. $|t|$ satisfies the same equation. So, in a situation where the reflection amplitudes at the junction for the two cases are taken to be equal then it follows from Eq. 8 that the TMR will be pinned to its maximum value *i.e.* magnitude of TMR $= 2$ and the temperature dependence will be flat even in the presence of inter-electron interactions.

Conclusions. – In this letter, we have studied both spin and charge transport in NSN, FSN, and FSF structures in the context of 1–D QW. We calculated the corrections to spin and charge transport arising from inter-electron interactions in the QW. We demonstrated the possibility for production of pure SC in such hybrid junctions and analysed its stability against temperature and voltage variations. Finally, we also showed that the presence of the CAR process heavily enhances the TMR in such geometries.

We acknowledge use of the Beowulf cluster at H.R.I. S.D. was supported by the Feinberg Fellowship Programme at WIS, Israel.